

## Research Article

Zhongling Tong, Qingtao Guan\*, Ahmed A. Abdou Elabbasy, Ali H. AlAteah, Ahmed M. Maglad and Mohammad Alharthai

# Empowering 3D printed concrete: discovering the impact of steel fiber reinforcement on mechanical performance

<https://doi.org/10.1515/rams-2025-0181>

Received September 25, 2025; accepted November 8, 2025;

published online December 11, 2025

**Abstract:** 3D concrete printing offers design freedom, eliminates formwork, reduces costs and waste, and accelerates construction, making it a powerful alternative to traditional methods. Reinforcing concrete during 3D printing remains a major challenge. Conventional reinforcement disrupts the extrusion process, while continuous methods using steel cables or wires face issues such as nozzle blockage, misalignment, and poor anchorage, limiting their effectiveness. Incorporating short, discrete fibers into 3DPCM provides self-reinforcement, simplifying the process while enhancing mechanical properties. However, including fibers affects the fresh state properties of 3DPCM, particularly the extrusion. This study reviews the effects of steel fibers addition on the fresh and hardened properties of 3DPCM by analyzing published literature results. Various journal articles are reviewed, and extracted data is summarized to identify the influence of steel fiber on flowability,

static yield stress, dynamic yield stress, printability, buildability, compressive strength and flexural strength of 3DPCM. The effect of steel fibers orientational distribution in printed filaments is also analyzed, and efforts to control the distribution to obtain favorable changes in the properties of 3DPCM are also highlighted.

**Keywords:** 3D concrete printing; steel fibers; mechanical properties; printability and buildability

## 1 Introduction

### 1.1 3D concrete printing

The construction industry needs to adopt technological innovations to remain competitive in a rapidly evolving environment. Implementing advanced technologies can boost productivity, elevate quality standards, reduce costs, and ensure efficient use of resources. Integrating advanced technologies such as digitalization, automation, artificial intelligence, and building information modeling (BIM) offers significant opportunities to enhance productivity, operational efficiency and economic viability. As part of the ongoing digital transformation, a suite of automated methods for concrete shaping has developed, encompassing digital casting, slipforming, and diverse forms of 3D printing [1–3]. Among these, the extrusion-based 3D concrete printing (3DCP) has recently gained notable attention from researchers and industry for its potential to reshape traditional construction practices [4–7]. 3D printing technology in construction offers several advantages over traditional construction. It allows for extensive design flexibility without requiring formwork and enhances construction efficiency by lowering labor costs, shortening construction timelines, and minimizing waste [8–12]. These potential advantages make 3DCP a compelling automated construction method for infrastructure development compared to traditional construction techniques [13].

**\*Corresponding author: Qingtao Guan**, Engineering Training Center of Changchun Sci-Tech University, Changchun, 130000, China, E-mail: [guanqingtao66@sina.com](mailto:guanqingtao66@sina.com)

**Zhongling Tong**, Engineering Training Center of Changchun Sci-Tech University, Changchun, 130000, China

**Ahmed A. Abdou Elabbasy**, Civil and Architectural Engineering Department, College of Engineering and Computer Sciences, Jazan University, P.O. Box 706, Jazan, 45142, Saudi Arabia. <https://orcid.org/0000-0002-8740-0108>

**Ali H. AlAteah**, Department of Civil Engineering, College of Engineering, University of Hafr Al Batin, Hafr Al Batin, 39524, Saudi Arabia

**Ahmed M. Maglad**, Department of Civil Engineering, College of Engineering, Najran University, Najran, 66462, Saudi Arabia. <https://orcid.org/0009-0002-9841-9100>

**Mohammad Alharthai**, Department of Civil Engineering, College of Engineering, Najran University, Najran, 66462, Saudi Arabia; and Science and Engineering Research Center, Najran University, Najran, 66462, Saudi Arabia. <https://orcid.org/0000-0002-3353-6202>

## 1.2 Role of fibers in 3DCP

Incorporating reinforcement into the concrete matrix during the printing process remains one of the most significant challenges to address for advancing the applications of 3D printing technology in construction. Conventional steel bar reinforcement is difficult to implement because the automated extrusion process is not designed to accommodate manual placement or embedment of rebar without interrupting the printing sequence. Continuous reinforcement strategies, such as inserting steel cables or wires during printing, have been investigated, but issues such as nozzle obstruction, misalignment, and lack of anchorage compromise efficiency [14]. The absence of standardized reinforcement strategies also hinders the adoption of 3DCP in structural applications, as current codes and design guidelines are tailored for conventionally cast reinforced concrete. The inclusion of fibers in the concrete matrix provides crack-bridging capability and residual tensile strength, thereby markedly improving the post-cracking behavior of concrete [15–17]. Adding short, discrete fibers to the printing materials offers promising potential due to its self-reinforcement capability, reducing complexity and time consumption [18, 19]. Research has demonstrated that inclusion of fibers in 3DPCM brings favorable improvements in its characteristics. Panda, Paul and Tan [20] reported that the mechanical properties of 3D-printed geopolymers improve with the incorporation of short glass fibers, with optimal enhancement observed at additions up to 1 % of the total weight. An experimental investigation was conducted on the flexural behavior of 3D-printed concrete reinforced with different lengths and dosages of steel fibers. The findings revealed that specimens incorporating 6 mm steel fibers at volume fractions of 0.75 % and 1 % exhibited the greatest improvement in flexural strength [21]. However, problems like fiber agglomeration, reduced printability, and anisotropy in mechanical response due to preferential fiber orientation during extrusion exist. Therefore, developing reinforcement approaches compatible with automated deposition, enhancing multi-directional strength, and ensuring structural reliability remains one of the foremost barriers to scaling 3DCP for load-bearing structures.

## 1.3 Scope and objectives of the review

This review paper examines the effect of steel fiber reinforcement on the fresh and hardened properties of 3DPCM. All aspects include a comprehensive literature synthesis of recent experimental work, emphasizing the effect of steel fiber type, geometry, volume fraction, and orientation on

fresh state properties such as workability, yield stress, extrudability and buildability of the 3DPCM. This review also critically evaluates the impact of fiber content, geometry, and orientation on the hardened state properties, including compressive and flexural strength. Particular focus is on establishing the trade-off between the printability and structural performance, because post-cracking behavior can usually be enhanced by fiber addition, but may be at the detriment of flowability and extrusion stability. The scope is limited to steel fibers, excluding other discrete reinforcements such as synthetic or natural fibers, in order to provide an in-depth understanding of steel fiber-concrete interaction within the 3D printing process. The main objective of the review is to identify optimum fiber dosages and configurations reported in the literature that balance printability and mechanical performance. Challenges and limitations associated with steel fiber integration in 3DPCM, including anisotropy, fiber clustering, and printability-performance trade-offs, are also discussed.

## 1.4 Research significance

The widespread adoption of 3DCP technology is still limited by key material shortcomings, particularly the brittle nature of cementitious materials and the lack of conventional reinforcement in printed elements. This review highlights the critical significance of steel fibers as a practical solution to these challenges. The significance of this review lies in the need to understand the effects of steel fiber addition on both fresh and hardened behavior of 3DPCM. Understanding these effects is important to bridging the gap between laboratory research and large-scale applications. This review explores how steel fibers affect rheology, printability, strength, cracking behavior, and durability, offering a clear guide for optimizing fiber-reinforced 3DPCM. These insights will help researchers, engineers, and industry professionals create better material mixes and design guidelines, supporting the wider use of 3D printing in construction.

# 2 Fundamentals of 3D printable concrete

## 2.1 Rheological requirements

In 3D concrete printing, the rheological requirements are contradictory. Concrete must exhibit high workability during pumping to facilitate extrusion, yet shift to low workability with high thixotropy afterwards to enhance

buildability [22–25]. Various research studies examined the relationship between the fresh and hardened properties of the mix and their impact on the robustness of the printing process, particularly in the context of large-scale adoption of concrete 3D printing [4, 26]. During deposition, the mix must retain its shape, which requires adequate yield stress in the fresh concrete. The thixotropic behavior of cement particles contributes to the buildup of yield stress at rest, enabling each filament to support subsequent layers [4]. The flowability of fresh concrete is influenced by the particle size distribution of the binder and sand, with a broader distribution proving more favorable [27, 28]. Achieving optimal print quality depends on the fresh properties of the mix in combination with the print path, which is primarily determined by the scale and complexity of the target geometry.

## 2.2 Mix design of steel fiber reinforced 3DPCM

For 3DPCM, the mix design is a key factor determining printability, strength, and durability of the printed element. It should be precisely tailored to provide adequate flowability and smooth extrusion through the printing nozzle. Mix design also affects the mechanical performance of printed concrete, such as its compressive strength, flexural strength, and durability. In 3DPCM, adding fibers requires a balance between flowability, extrudability, and buildability, making it essential to identify optimal mix proportions. Traditional mix design methods for conventional concrete are unsuitable for 3DPC. Although recent studies have proposed empirical approaches, a standardized mix design method has not yet been established because of the limited research and application history of 3DPC. In many cases, mixture proportions are reported without a clear design methodology or explanation of how the parameters were determined [29, 30]. Most 3DPCM uses a fine-aggregate mortar-like mix with no coarse aggregates. Instead of traditional slump-based workability testing, rheology-based and extrusion tests are used to proportion the mix. Superplasticizers enhance flowability without increasing water content, while viscosity-modifying agents are commonly added to prevent segregation. Accelerators or retarders are used to regulate the setting time [31]. Recent studies agree that 3DPCM mix design requires iterative optimization, where material composition (binder type, fine aggregates, SCMs, fibers) and admixture dosage are balanced to meet three key properties, namely extrudability, buildability and interlayer bond strength, with extrudability and buildability being the most important fresh state properties [29, 32]. (Table 1).

## 3 Effects on fresh properties of 3DCM

### 3.1 Flowability

Incorporating steel fibers into 3D printable concrete mixtures significantly influences their rheological behavior, particularly in terms of flowability. In the fresh state, 3DPCM requires a delicate balance between adequate flow for extrusion and sufficient buildability for layer stability. Due to their high stiffness and aspect ratio, steel fibres interact with the cementitious matrix through mechanical interlocking and frictional drag, which generally increases resistance to flow [44–46]. Xia, Geng [38] observed a significant decrease in the flow diameter of 3DPCM as fiber content increased from 0.1 to 0.9 %. This effect is more pronounced with longer steel fibers [38]. Longer fibers are more prone to bridging and entanglement, which increases resistance to flow, especially in narrow flow channels during the spread test. They also increase the likelihood of fiber clustering. The effect of steel fibers on flow diameter, as reported in the literature, is presented in Figure 1. It can be observed that in almost all studies, the inclusion of steel fibers reduced the flow diameter. However, the reduction rate varies significantly between studies due to differences in fiber length, geometry, aspect ratio, mix design, and superplasticizer dosage. In some studies, such as Xia (2025), effect is high, whereas in some studies such as Zhang, Zhu [47] and Singh, Liu [48], it is moderate or even flat curve is observed by Chen, Li [43]. Possible reason for sharp decrease in Xia's results may be the absence of a viscosity modifier. In investigations, where viscosity modifier was used, the inclusion of fibers didn't affect flow diameter significantly. The observed differences across studies underline the importance of tailoring fiber dosage and mix design to the printing system's specific requirements, especially the optimized utilization of the viscosity modifier.

### 3.2 Static yield stress

The inclusion of steel fibers affects the fresh mix's yield stress and plastic viscosity. Higher fiber content typically increases both, which can improve buildability but may hinder extrudability. Jia, Zhou [40] investigated how different shapes and amounts of steel fibers affect the rheological characteristics of fresh mixtures. As shown in Figure 2(a), the static yield stress of the fresh mixture was found to increase with higher fiber content, with a more pronounced rise observed beyond 1.0 vol% steel fibers. Up to

**Table 1:** Mix proportions used for steel fiber reinforced 3DPCM.

Binder content (kg/m <sup>3</sup> )		Aggregate (kg/m <sup>3</sup> )	Aggregate/ binder	Steel fibers content kg/m <sup>3</sup> (vol%)	Fiber length (mm)	Water kg/m <sup>3</sup>	SP <sup>a</sup> kg/m <sup>3</sup> (%)	VM <sup>b</sup> kg/m <sup>3</sup> (%)	Ref.
OPC	SCM								
750	330	1,080	1	78 (1)	6, 10	154	10	1.08	[33]
483	590	1,074	1	58.9 (0.75)	6	182	–	–	[34]
802–818	–	1,122–1,145	1.4	77–153 (0–2)	13	280–286	(0.018–0.130)	–	[35]
746–760	75–76	1,148–1,177	1.4	77–153 (1–2)	13	261–266	(0.16–0.32)	–	–
750	330	1,080	1	19.5–78 (0.25–1.00)	6, 10	154	10	1.08	[36]
798–818	–	1,117–1,145	1.4	39–190 (0.5–2.5)	13	279–286	(0.02–0.22)	–	[37]
712–726	–	1,281–1,306	1.8	39–153 (0.5–2.0)	13	249–254	(0.09–0.27)	–	–
725	75	1,000	1	(0.1–0.9)	6, 9, 12	260	6 (0.06)	–	[38]
694	231	1,180	1.3	(1.5–3.0)	35	192	(1.5)	(0.25–0.50)	[39]
843	590	1,074	0.75	19.6–78.5 (0.25–1.00)	3, 6	182	10.7 (1)	–	[21]
630	270	900	1	(0.5–1.5)	13	180	5.94	–	[40]
2,000	–	2000	1	(0.25–0.75)	25	440	10	(0.25)	[41]
758	200	1,027	1.07	(0.5)	13	230	–	–	[42]
788	200	1,100	1.1	78–234 (1–3)	3.3–17.8	138–177	10	(0.5–2.0)	[43]

<sup>a</sup>Super plasticizer. <sup>b</sup>Viscosity modifier.

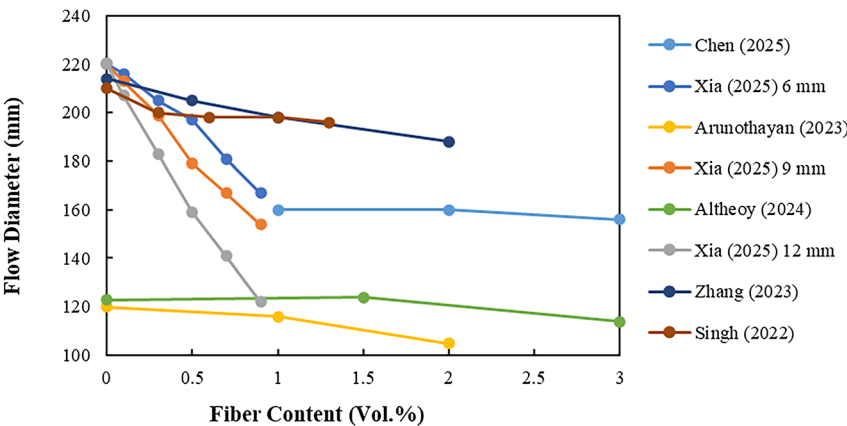


**Figure 1:** Effect of steel fiber content on flow diameter of 3DPCM [38, 39, 43, 47–49].

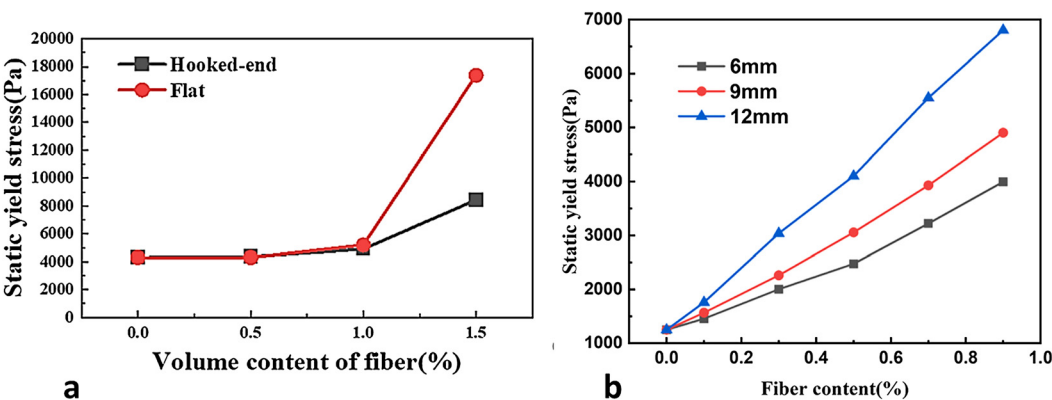


**Figure 2:** Effect of steel fiber content on static yield stress of 3DPCM as reported by (a) Jia, Zhou [40]; (b) Xia, Geng [38].

1.0 vol%, fibre shape didn't affect static yield stress much but above this, flat end fibers resulted in a more prominent increase than hooked-end fibers. However, in another study by Xia, Geng [38], a significant increase in static yield stress was observed even at lower fiber dosage (<1.0 %) (see Figure 2(b)). It was also observed that increasing the fiber length from 6 mm to 12 mm sharply increased static yield stress. It may be possible that longer fibers span larger matrix volumes, increasing mechanical obstruction during flow. This results in higher internal resistance, reflected as increased yield stress. Authors argued that incorporating steel fibers generates a three-dimensional framework within the concrete, similar to scaffolding, which impedes the material's flow and elevates its static yield stress. Unlike Jia's results, there's a consistent linear trend suggesting that fiber length affects rheology more predictably than fiber geometry.

### 3.3 Dynamic yield stress

Dynamic yield stress is the minimum stress required to initiate flow under shearing conditions (typically during pumping or extrusion). Steel fibers increase the dynamic yield stress of 3DPC proportionally to their content, length, and aspect ratio. While beneficial for mechanical integrity, this effect can significantly impair printability beyond certain thresholds. Arunothayan, Nematollahi [49] evaluated the yield stress buildup of 3DPCM with varying fiber content, i.e. 0 %, 1 % and 2 %. Steel fiber inclusion in 3DCP led to a marked increase in static yield stress at all resting periods, as shown in Figure 3. This increase is largely due to the rigidity of the steel fibers, which reinforce the composite's internal resistance to flow. Substantial yield stress

increase at 2 % fiber content suggests aggressive thixotropic stiffening. The high initial resistance may have resulted from fiber entanglement, surface friction, and alignment effects.

The variation of dynamic yield stress with increasing fiber content, as reported in various research studies, is shown in Figure 4. At lower fiber contents (0–1 vol%), in the studies of Altheoy, Zaid [39] and Arunothayan, Nematollahi [49] show low yield stress values. However, beyond 2 vol%, a sharp increase is evident. The results of Xia, Geng [38] show a positive linear correlation between fiber content and dynamic yield stress at all fiber lengths. However, increased fiber length has a more significant effect, likely due to forming a more interconnected network that increases internal friction and resistance to flow. Differences in aspect ratio, stiffness, or surface texture may be the reason for such diverse trends. Longer or more rigid fibers increase yield stress due to higher entanglement and the blockage effect. Different base mixes (cement content, additives like silica fume, viscosity modifiers) may also affect the ability of fibers to alter rheology. Yield stress increases with fiber content, but the rate and threshold of increase are study-specific, influenced by fiber length, mix design, and processing.

### 3.4 Printability

Printability of 3DPCM is referred to the ability of a cementitious mixture to be smoothly extruded, maintain its shape after deposition, and build up multiple layers without collapse or deformation. Despite the absence of standardized guidelines for evaluating the printability of 3DPCM, extrudability and shape stability are commonly acknowledged in the literature as essential criteria for characterizing the printability of cementitious mixtures [50–52]. Steel fibers can improve shape retention by increasing cohesion. However, excessive fiber content often leads to nozzle clogging and discontinuities in printing. It should be kept in mind that the balance between stiffening and flowability is essential for successful layer deposition.

The dosage of steel fibers has a critical and nonlinear effect on the printability of 3DPCM. Altheoy, Zaid [39] observed improved buildability and sufficient extrudability when using double-hooked steel fibers at 0.75 % in ultra-high-performance 3DPC. Li, Wei and Khayat [53], evaluated the extrudability of fiber reinforced 3DPCM by printing a single layer of 300 mm length and 40 mm width with various fiber volume contents ranging from 0.5 % to 2.5 %. It was revealed, as shown in Figure 5, that the filament with 2 % 6-mm steel fibers was extruded continuously and without clogging, maintaining a shape consistent with the desired width. At 2.5 % steel fiber content, the filament exhibited

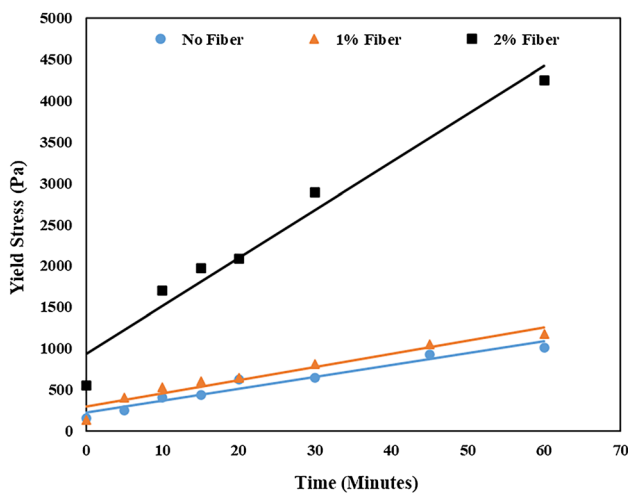


**Figure 3:** Effect of fibers on yield stress buildup of 3DPCM with rest time [49].



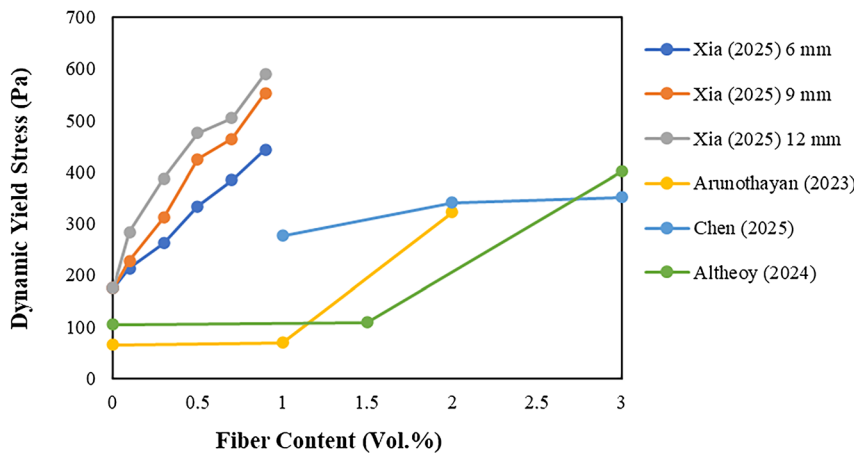


**Figure 4:** Dynamic yield stress versus varying fiber content [38, 39, 43, 49].

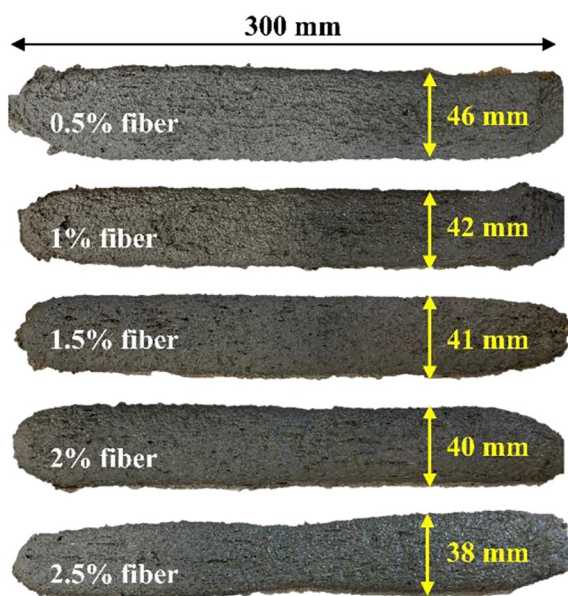


**Figure 5:** Effect of steel fiber content on width of printed filament [53].

significant irregularities and interruptions, likely caused by nozzle clogging due to the high fiber concentration. Increased fiber volume restricts flow and promotes physical interlocking, making clogging more probable [53].

Xia, Geng [38] reported that 0.9 vol% steel fibers resulted in a more uniform filament width than polypropylene and basalt fibers (see Figure 6). They argued that the higher rigidity of steel fibers compared to polypropylene and basalt fibers is responsible for smooth extrusion due to the reduced possibility of clump formation. It was also noted that the increase in fiber content resulted in filament width closer to the designed initial width. This may be attributed to the interlocking effect of fibers and reduced fluidity.

To evaluate the buildability of 3D printed cementitious materials (3DPCM), researchers employ various methods, with the layer stability test being one of the most common

and straightforward approaches. Some researchers have described the layer stability as the percentage of deformation in the bottom layer caused by the weight of the subsequent layer on top of it. At the same time, other researchers regarded shape stability as the deformed height as a percentage of the initial height of all printed layers. Zhang, Zhu [47] observed that shape stability improves with higher steel fiber content, reaching 80.0 % shape retention at 2.0 % fibers compared to 43.0 % in the control mix. This enhancement is attributed to greater interlocking between steel fibers and aggregates, forming a denser and more rigid skeletal network that enhances the deformation resistance of the 3DPCM.

However, in another study, the opposite trend was observed, as shown in Figure 7, where increasing the fiber dosage resulted in increased deformation of the bottom layer (18 % with 2.5 % fiber vol. compared to only 5 % of the control mix) [37]. It is important to note that the higher deformation in fiber reinforced 3DPCM may be due to a higher dosage of water reducing agent used to counter the negative effects of steel fiber on flow properties. In the study of Zhang, Zhu [47], the amount of water reducing agent was kept constant across all fiber contents. Additionally, higher sand-to-binder ratios of 1.4 and 1.8 were used by Giwa, Game [38], compared to 1 used by Zhang, Zhu [47].

The outcomes of various research studies that evaluated the effects of steel fibre content on printability are summarized in Table 2.

The printability of 3DPCM incorporating steel fibers is significantly influenced by fiber length due to its effects on rheology, extrusion, and interlayer bonding. Shorter fibers generally enhance smooth extrusion and minimize nozzle clogging, whereas longer fibers improve layer interlocking but may induce fiber entanglement and reduce flowability. Yang, Wu [36] observed that adding 1 vol% of 6 mm fibers slightly reduced uniformity but still maintained a close layer

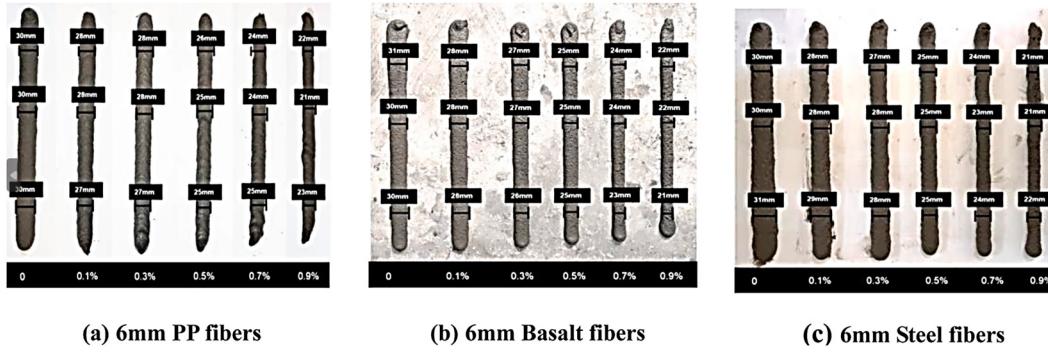


Figure 6: Extrudability of 50 cm long filament with different types of fibers [38].

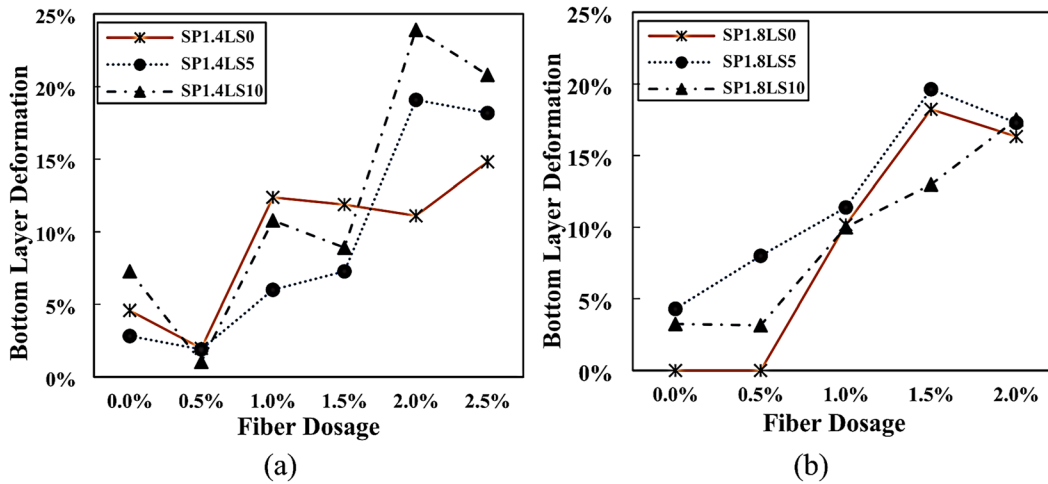


Figure 7: Effect of steel fibers on bottom layer deformation (a) sand/binder = 1.4 (b) sand/binder = 1.8 [37].

thickness ( $5 \text{ mm} \pm 0.5 \text{ mm}$ ), though minor pits appeared due to nozzle drag. When 10 mm fibers were used at the same volume, extrusion became more uneven due to greater

difficulty in extracting the mortar through the nozzle, with fibers occasionally clumping and extruding together, leading to inconsistent layer thickness as observable in Figure 8.

Table 2: Summary of steel fiber effects on printability parameters.

Fiber content (vol%)	Extrudability parameter	Buildability parameter	Effect on extrudability	Effect on buildability	Optimum fiber dosage	Ref.
0.5–2.5 %	300 mm long filament with consistent width (40 mm)		Positive		2 %	Li, Wei and Khayat [53]
0.5–2.5 %	–	Shape retention rate (%)	–	Positive	2 %	Zhang, Zhu [47]
0.5–2 %	–	Bottom layer deformation	–	Negative	–	Giwa, Game [37]
0.1–0.9 %	50 cm long filament with consistent width (20 mm)	Height loss rate (%)	Positive	Positive	–	Xia, Geng [38]
2 %	250 mm long filament with consistent width	Shape retention ability index	Positive	Positive	2 %	Arunothayan, Nem-atollahi [54]
0.5–1.5 %	300 mm long filament with consistent width (40 mm)	Height of 8 layers	Positive	Positive	1 %	Jia, Zhou [40]

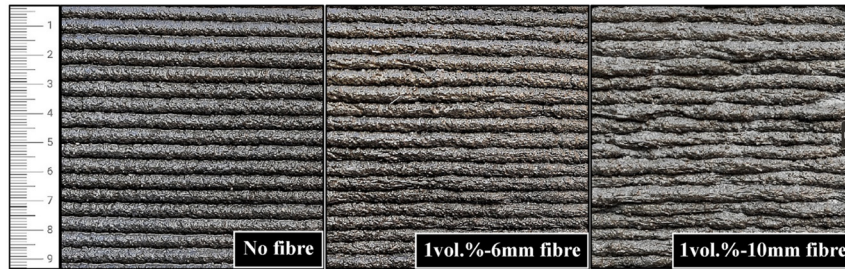


**Figure 8:** Effect of steel fiber length on printability of 3DPCM [36].

Xia, Geng [38] also observed that steel fibers longer than 15 mm led to intermittent nozzle clogging, while fibers less than 10 mm length maintained continuous filament flow with minimal defects.

## 4 Effects on hardened properties of 3DPCM

### 4.1 Compressive strength

Incorporating steel fibers into 3DPCM has a distinct impact on compressive strength, primarily influenced by fiber volume fraction and the interaction between fibers and the matrix. Most published studies report an enhancement in compressive strength of 3DPCM with the addition of short steel fibers. Because printed specimens are produced without vibration and formwork, so their compressive strength is lower than traditionally mold-cast specimens. Generally, the compressive strength of 3DPCM enhances when fibers are utilized at an optimum volume percentage, which ranges between 0.5 % and 2 %. The higher fiber contents (>2.0 %) can reduce strength due to poor dispersion, fiber clustering, and increased porosity. Due to the inherent anisotropic behavior introduced during the 3D printing process, the compressive strength of 3DPCM is usually determined by loading applied along 3 different directions. Although different research studies intend to define

independent loading directions, in this review study the loading directions defined are presented in Figure 9. Loading direction X is defined as when load is applied along the printing plane and perpendicular to print/layer direction. When load is applied along the printing plane and parallel to print/layer direction, it is defined as loading direction Y. Whereas, the loading direction Z is defined as the load applied normal to printing plane. If, in any research study cited here, the loading direction is defined different from this definition, it is converted to match the definition defined here.

As reported in the literature, the effects of varying steel fiber content on the compressive strength of 3DPCM are summarized and presented in Figures 10–12. The plot reveals significant variability in the influence of steel fiber content on compressive strength across different studies. It can be observed that in most of the studies, the incorporation of steel fibers tends to increase the compressive strength of 3DPCM. Zhang, Zhu [47] explains that, when a crack is initiated, the stress is transferred from the cement-based matrix to the fibers, which helps arrest crack propagation and enhances compressive strength through the fiber pull-out mechanism. As the fiber content increases, the spacing between fibers decreases, leading to greater fiber overlap and increased friction. This further restricts crack growth and contributes to improved compressive strength.

Singh, Liu [48] reported that the compressive strength is higher in the Z direction than in the X and Y directions due to the horizontal layers functioning like small beams stacked

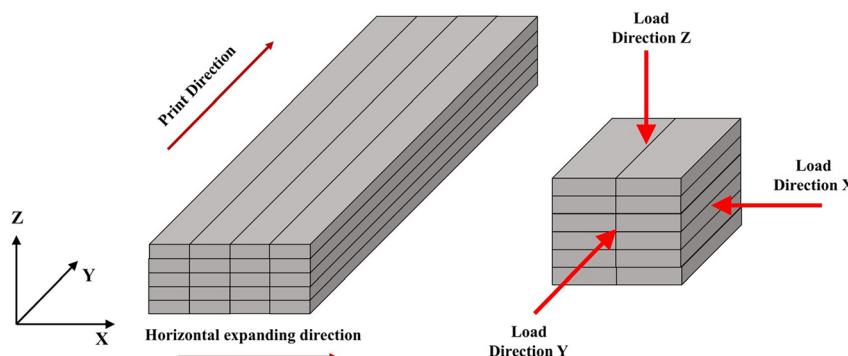


**Figure 9:** Loading directions for compressive testing defined in this review study.



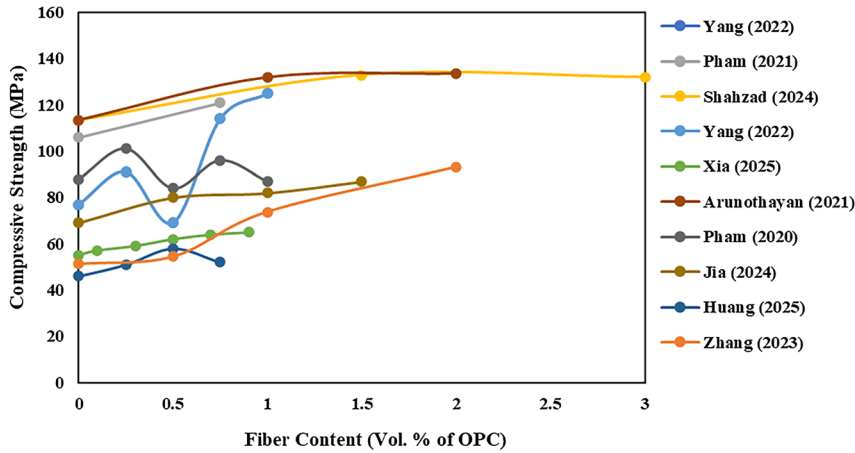


**Figure 10:** Effect of steel fiber content on compressive strength in X direction [21, 33, 34, 36, 38, 40, 41, 47, 55, 56].

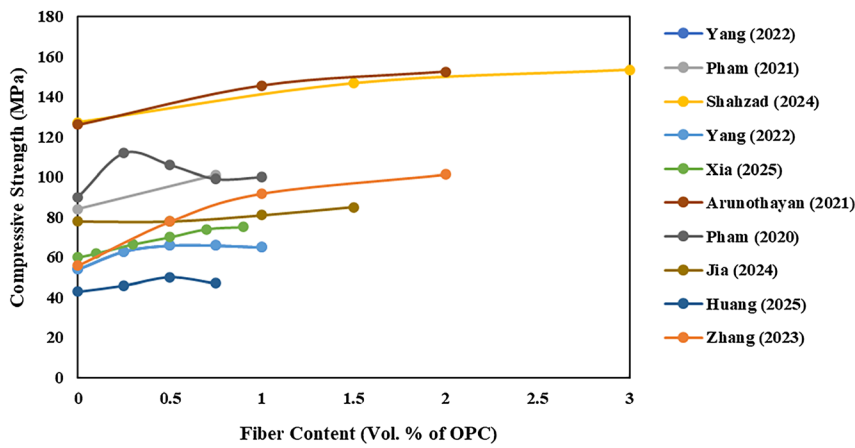


**Figure 11:** Effect of steel fiber content on compressive strength in Y direction [21, 33, 34, 36, 38, 40, 41, 55, 56].

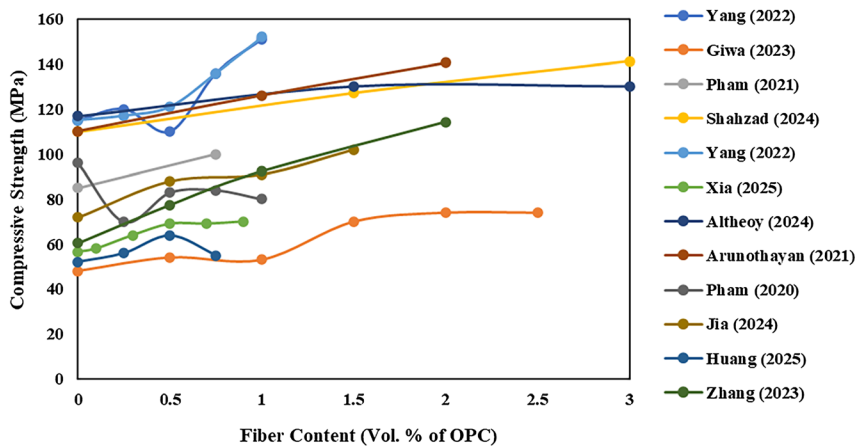


**Figure 12:** Effect of steel fiber content on compressive strength in Z direction [21, 33–41, 47, 55, 56].

vertically, allowing the load to be distributed over a larger area. Another key factor is the interlayer adhesion, which can enhance the concrete's overall strength by improving the bonding between layers. Fibers can form an energy-absorbing mechanism through mechanical anchorage, contributing to higher compressive strength and better structural integrity. Research by Giwa, Game [37] and Xia,

Geng [38] shows an initial increase followed by a plateau, particularly beyond 1.5–2.0 % fiber content. This indicates a saturation point, beyond which fibers no longer contribute significantly or even impair performance due to clustering, workability loss, or void formation.

Figure 13 shows the percentage improvement in compressive strength of 3DPCM due to fiber reinforcement.

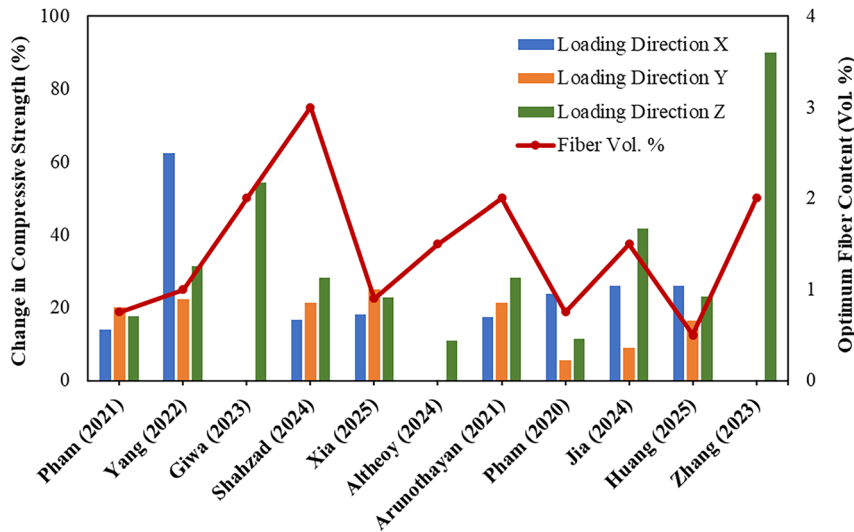


**Figure 13:** Percentage improvement in compressive strength and optimum fiber content [21, 33–41, 47, 55, 56].

The optimum fiber content values are also plotted. It can be observed that the Strength gain varies significantly with loading direction, suggesting that the alignment or orientation of fibers within the matrix plays a crucial role. A non-linear relationship is evident between fiber content and strength gain. While some increase in fiber volume results in higher strength, saturation or inefficiency appears beyond 2.5–3 %. It can also be noted that the loading Direction Z is the most favorable for compressive strength enhancement, likely due to better load transfer through fiber alignment.

Optimum fiber content lies between 1 % and 2 %, balancing mechanical benefit and material workability. However, in the case of 3DPCM, steel fiber content alone is not a deterministic factor. Its interaction with print process, material design, and fiber characteristics governs compressive strength outcomes.

## 4.2 Flexural strength

Steel fiber inclusion in 3DPCM consistently enhances flexural strength by improving crack-bridging, post-crack load capacity, and energy absorption. Across studies, the magnitude of improvement depends on fiber dosage, geometry, and distribution within the printed layers. As shown in Figure 14, most studies show an increasing trend in flexural strength with higher steel fiber content, confirming that steel fibers enhance crack-bridging and post-crack load resistance. It can be observed that the high flexural strength of 45 MPa was achieved by Yang, Wu [36] with the inclusion of 1 vol% steel fibers. Shahzad, Abbas [56] also observed a constant increase in flexural strength reaching 40 MPa at 3 vol%. This curve suggests the mix tolerates very high fiber loading with minimal workability loss. Studies, including

those by Yang, Wu [36], observed an initial increase up to a dosage of 0.5 vol% followed by a decline at higher dosages. It was observed that the flexural strength of high-strength or ultra-high-strength mixes, such as Yang, Wu [36] and Shahzad, Abbas [56], increased more steadily compared to normal strength mixes due to better anchoring of fibers in a dense matrix. Conventional mixes [37, 57] start low, and the strength gain is limited even with fibres.

The percentage improvement in flexural strength and corresponding fiber volume content from various studies is presented in Figure 15. It can be observed that the gain in flexural strength is more pronounced than in compressive strength. The optimum fiber content to achieve the highest flexural strength varies across studies. Shahzad, Abbas [56] study shows the highest gain in flexural strength with 3 vol% steel fibers. While other researchers observed significant improvement in flexural strength at lower dosages as well such as 0.5 % fiber yielded a ~50 % increase, suggesting that baseline material was relatively weak and therefore benefited noticeably from a small amount of crack-bridging reinforcement. Several factors, such as optimized rheology, consistent fiber orientation during extrusion, and strong interfacial bonding between fibers and cement paste, affect the performance of fiber-reinforced 3DPCM.

## 4.3 Post-crack behavior

Steel fibers are known to improve the post crack performance of concrete significantly. In 3DPCM, cracking is often governed by weak interlayer bonding and the brittle nature of the cementitious matrix. Unlike cast concrete, where reinforcement is embedded continuously, 3DPCM relies heavily on fiber reinforcement to improve ductility and

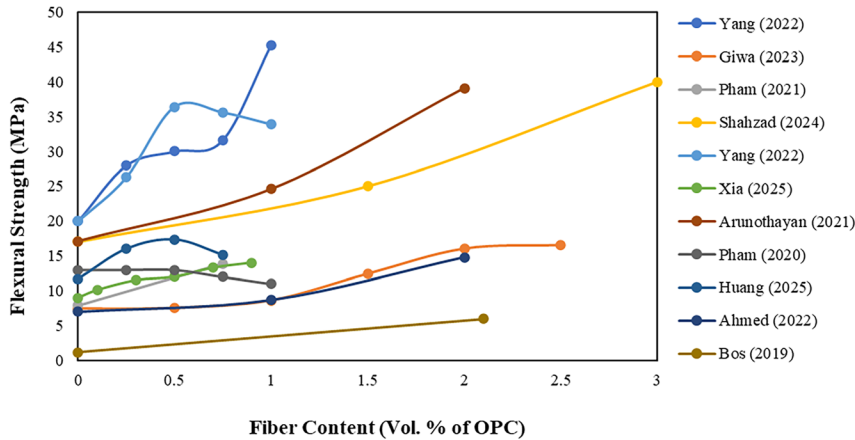


**Figure 14:** Effect of steel fiber content on flexural strength of 3DPCM [21, 34–38, 41, 55–57].

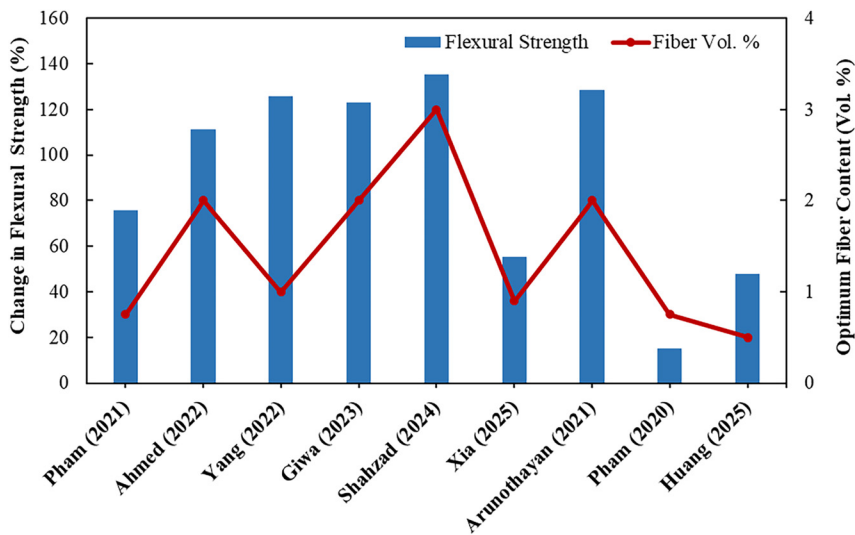


**Figure 15:** Percentage improvement in compressive strength and optimum fiber content [21, 34–38, 41, 55–57].

toughness. The inclusion of steel fibers has been shown across multiple studies to transform brittle post-cracking failure into a more ductile, energy-absorbing behavior. However, the degree of improvement depends strongly on fiber content, orientation, and distribution. Without steel fibers, brittle fracture behavior was observed in 3DPCM samples by Zhang, Zhu [47] as compared to fiber reinforced 3DPCM. As shown in Figure 16(a), there is minimal residual strength and essentially no capacity to carry load after peak, confirming that plain 3DPCM behaves like a typical quasi-brittle cementitious material with poor crack resistance. However, adding 0.5 % steel fibers significantly modifies the curve (Figure 16b). The post-crack response shows a slight plateau after the peak load, indicating the crack bridging effect. This effect is more pronounced at higher fiber dosage as indicated by the strain-hardening response in Figure 16c and d, where load-carrying capacity after cracking is maintained and sustained over extended deflections. This

performance confirms that higher fiber volume significantly enhances ductility and toughness.

Similar findings were reported by [54] (shown in Figure 17), where both mold cast and 3DPCM matrix (without fibers) display sudden failure with negligible post-peak capacity. This reflects the brittle nature of matrix. Whereas the composite, i.e. with inclusion of fibers, exhibits enhanced post-crack behavior. It is evident that fibers fundamentally change the post-crack response. While all matrix specimens fail abruptly, composites exhibit ductile behavior with significant energy absorption. Steel fibers dramatically enhance flexural strength and ductility, converting brittle failure into ductile, strain-hardening behavior.

However, challenges remain with anisotropy (orientation along print path) and printability at higher dosages. Still, overall, steel fibers provide the most practical reinforcement solution for improving the structural reliability of 3DPCM in its post-cracking regime.

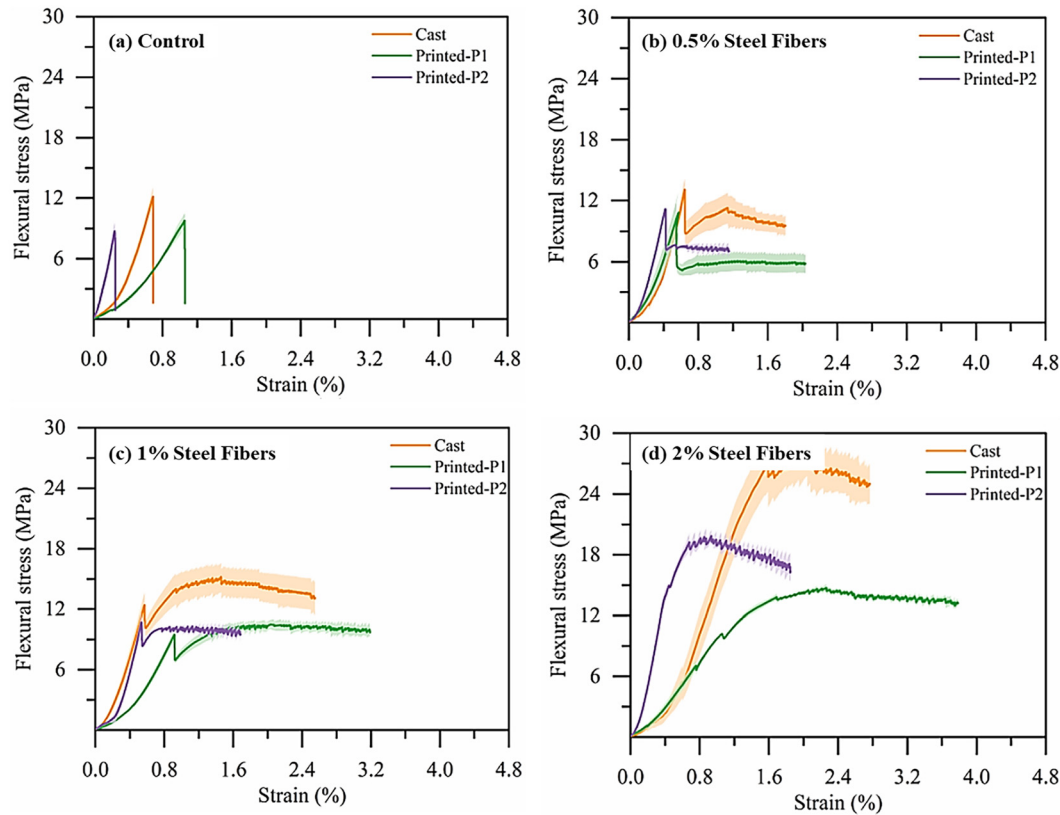


**Figure 16:** Effect of steel fibers on post-crack performance of 3DPCM (a) without fibers; (b) with 0.5 % steel fibers; (c) 1.0 % steel fibers; (d) 2.0 % steel fibers [47].

#### 4.4 Microstructure

The microstructural analysis of steel fiber reinforced 3DPCM, primarily focusing on the interfacial transition zone (ITZ) between the fiber and cementitious matrix, is very important for understanding performance. A strong ITZ

means fibers can develop full pull-out resistance, directly improving flexural strength, toughness, and post-crack ductility. In 3DPC, extrusion flow can cause preferential fiber orientation and may even trap micro-voids around fibers, weakening the ITZ compared to cast concrete. This fact was observed by Jia, Zhou [40] as shown in Figure 18. During

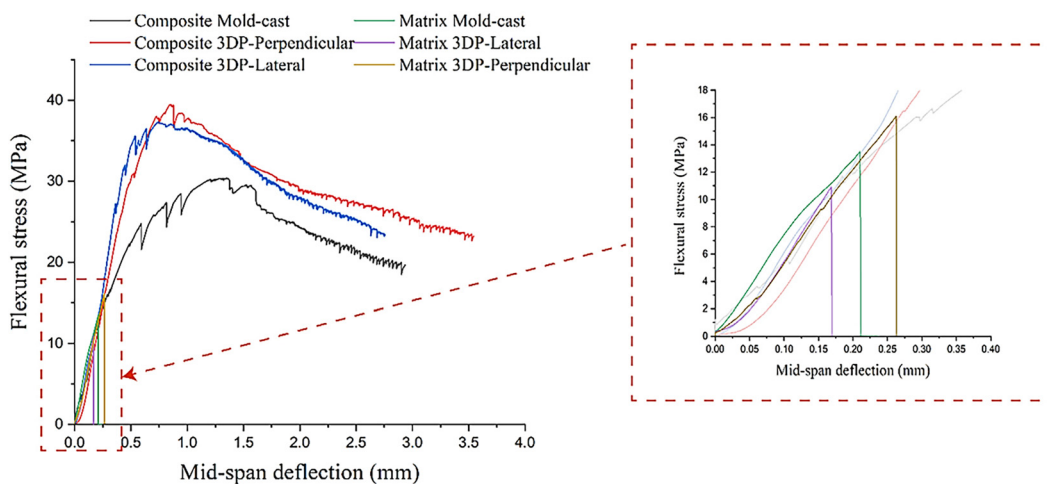


**Figure 17:** Comparison of post-crack behavior of 3D printed matrix (without steel fibers) and composite (with steel fibers) [54].



extrusion, mismatched movement between the fibers and the mortar matrix can lead to the formation of gaps around the fibers, particularly in the case of hooked-end fibers. However, the formation of gaps in the ITZ may also be influenced by the preparation process, particularly factors such as the exact cutting position of steel fibers and the methods employed for cutting and polishing. Further investigation is warranted to validate this observation.

In a research study, using a mineral modifier (blend of sand, clayey rocks and chalk) was reported to have improved the fiber-matrix ITZ [58]. In the obtained fiber-reinforced concrete, the interfacial transition zone appeared as a cohesive monolith, free from pores, voids, cracks, or cavities. It was marked by strong fiber-to-matrix adhesion, further densified by newly formed hydration products, as shown in Figure 19. Consequently, the mineral modifier markedly enhances the bond between the hardening binder and the fibers.

Xia, Geng [38] noted from microanalysis that the steel fibers exhibit a pull-out behavior during flexural failure as compared to rupture of basalt fibers evident from Figure 20. Authors argued that unlike PP and basalt fibers, steel fibers tend to fail through pull-out rather than rupture because of their higher stiffness and strength. This stronger mechanical interlocking with the cement matrix enhances the overall mechanical performance of the specimens. The

pronounced interlocking effect dissipates considerable energy during cracking, providing a substantial reinforcement contribution.

## 5 Fiber orientational distribution in printed layers

In 3DPCM, the layer-by-layer extrusion process tends to align fibers along the nozzle's movement, allowing fiber orientation to be controlled through toolpath design as explained by Zhou, Lai [59] in Figure 21. The authors emphasized that the directional distribution of steel fibers significantly affects the mechanical properties of 3DPCM. Furthermore, they highlighted the presence of a distinct interfacial structure in 3DPCM, which also plays a critical role in determining its mechanical performance. They observed that compressed specimens sustained damage at the side surfaces, as indicated by fracture patterns. Tensile stresses developed at these side surfaces during compression, so the tensile strength of near-surface regions is a key factor controlling the specimens' compressive strength.

This anisotropy creates directional dependence in mechanical performance i.e. flexural and tensile strength

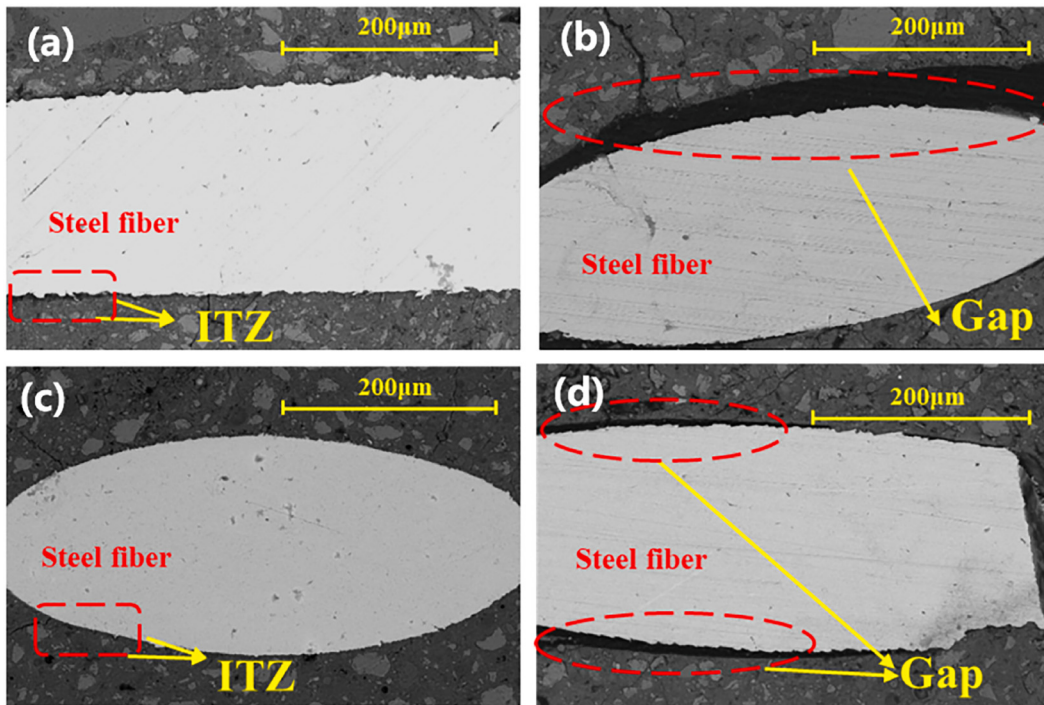


**Figure 18:** Morphology of steel fiber-matrix ITZ: (a) Mold cast with hooked fibers; (b) 3DPC with hooked fibers; (c) mold cast with straight fibers (d) 3DPC with hooked fibers [40].

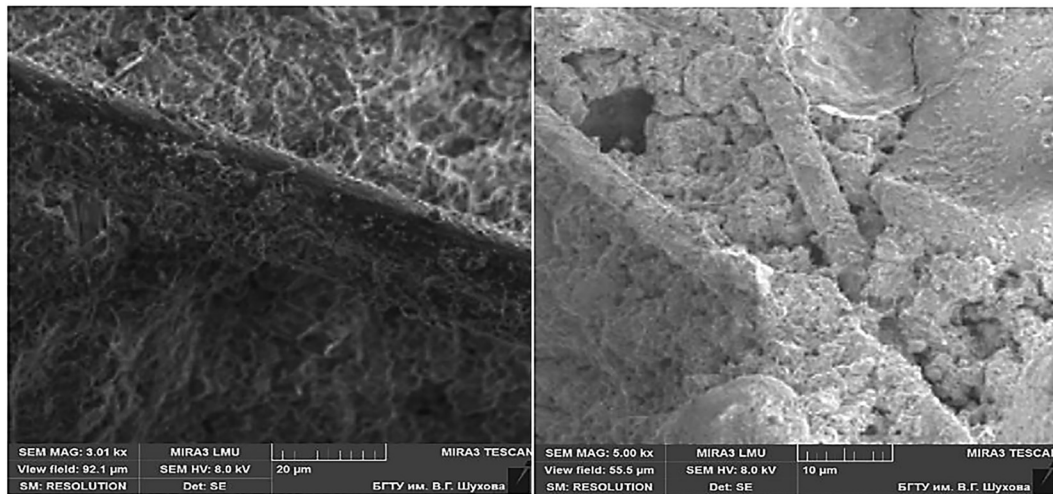


Figure 19: Fiber-matrix ITZ with mineral modifier in 3DPCM [58].

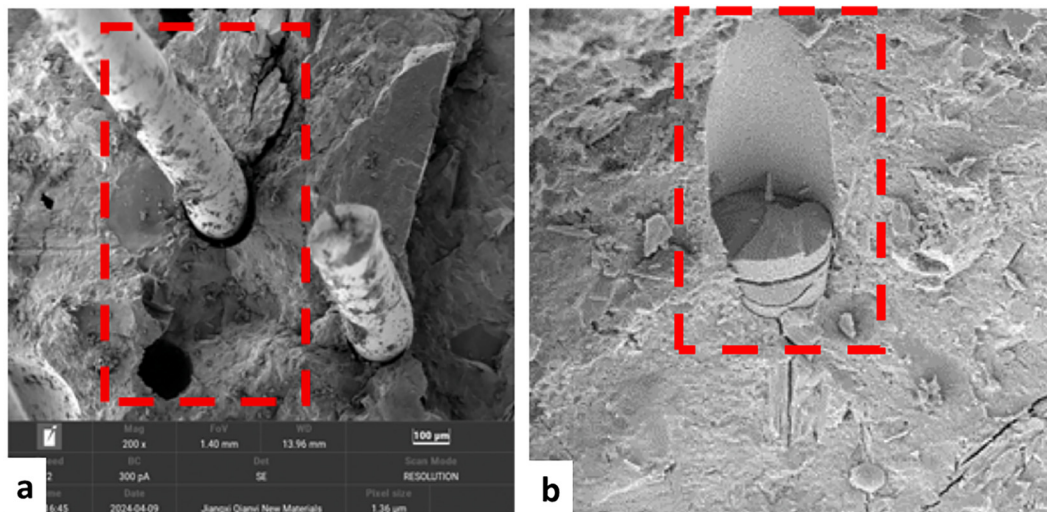


Figure 20: Micromorphology of fiber-3DPCM matrix ITZ after failure: (a) Pullout of steel fibers; (b) rupture of basalt fibers [38].

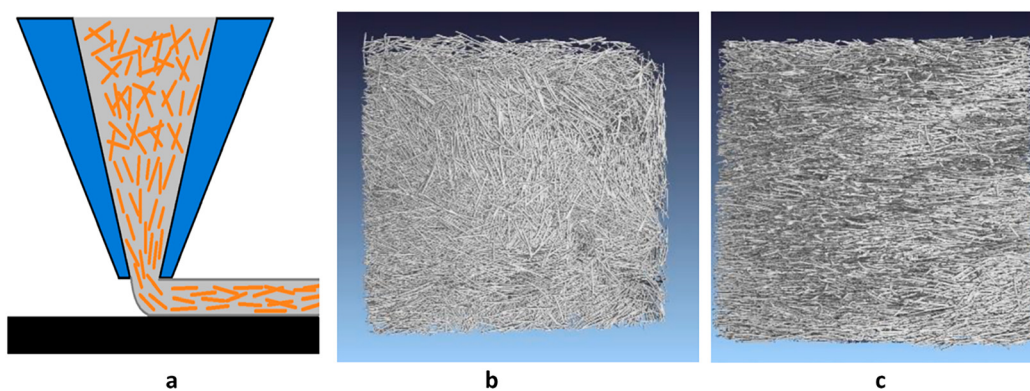
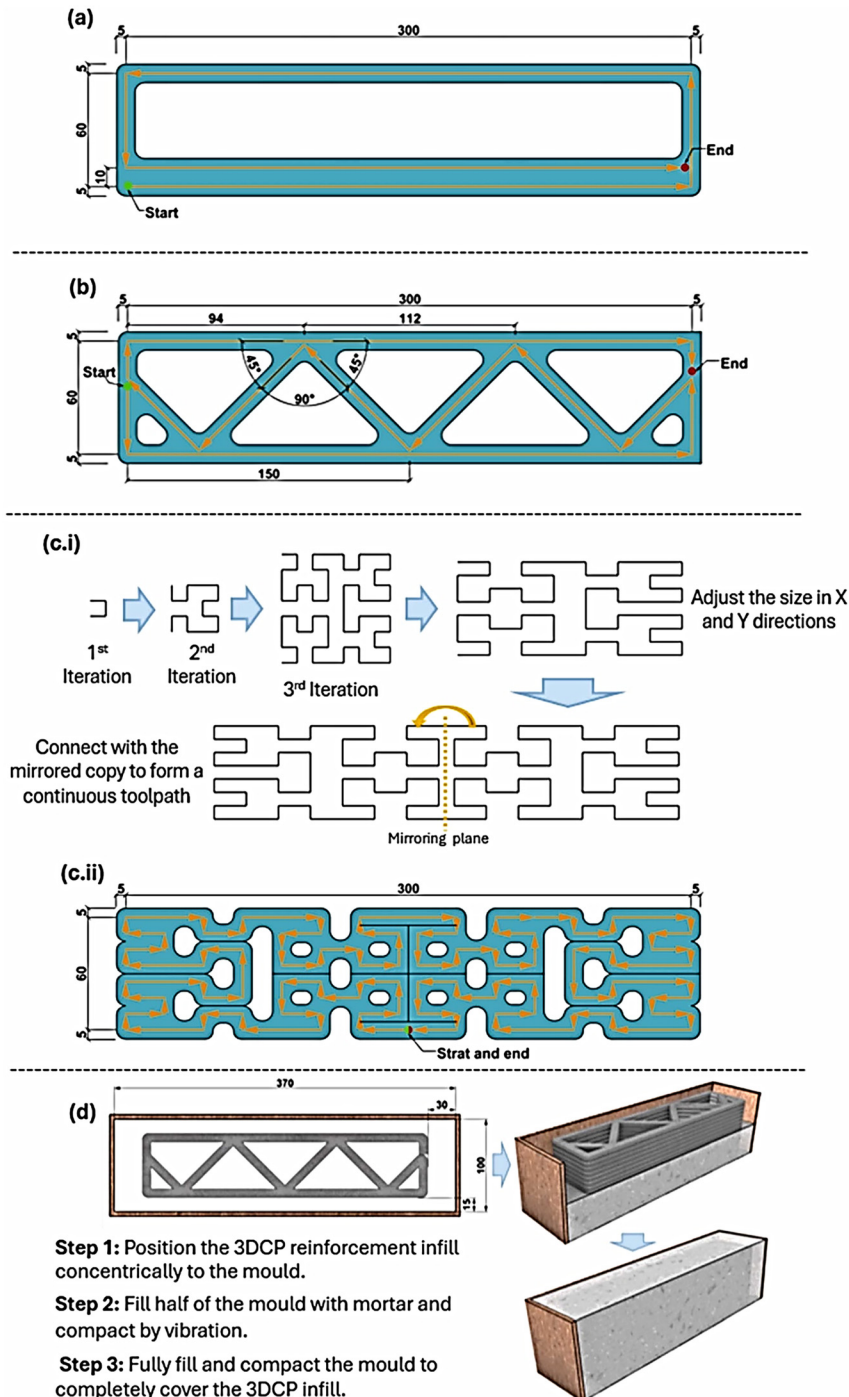


Figure 21: Alignment tendency of steel fibers along print direction: a) Schematic of fiber alignment during extrusion; b) CT scan of mold cast sample; c) CT scan of ed printed sample [59].

are highest along the print path but weaker across layers. The crack-bridging capability of fibers depends strongly on their orientation. For example, aligned fibers provide effective resistance along their axis, while randomly oriented fibers distribute toughness more evenly across directions. It is also important that fibers aligned parallel to layers may not effectively bridge across weak interfacial planes, which is a key failure mode in 3DPC. Li, Khieu

[16] proposed a two-scale strategy utilizing 3D printing to regulate fiber orientation and distribution in cement composites. The study demonstrated notable improvements in flexural strength and toughness through tailored reinforcement patterns, with steel fibers arranged in a rectangular infill configuration as shown in Figure 22, achieving over a 100 % increase in flexural strength.



**Figure 22:** Steel fibers arranged in a rectangular infill pattern proposed by Li, Khieu [16].



Huang, Peng [41] magnetic field application controls steel fiber alignment within the fresh concrete during extrusion. CT scanning and image analysis confirmed that fibers subjected to a magnetic field showed significantly higher degrees of alignment than extrusion-driven orientations. Specimens with magnetic orientation showed more balanced performance across different loading directions than extrusion-only orientation, which favored the print path. X-ray CT images in Figure 23 show that fibers largely retain their extrusion-driven orientation with low field intensity, resulting in a lower orientation index. The authors noted that with increased magnetic field intensity, fibers realign effectively, bridging cracks in multiple directions and improving flexural performance, especially across interlayers.

However, too close placement of the magnet to achieve higher field intensity may not be feasible in practical large-scale printing due to physical constraints, non-uniformity of the field, and the difficulty of ensuring consistent exposure across thicker elements. Fiber orientational distribution is a critical factor influencing the structural performance of 3D printed fiber-reinforced concrete and must be carefully considered in both experimental evaluation and practical applications.

## 6 Discussion

Use of steel fibers in the 3DPCM benefits in various aspects, as shown in Figure 24. Steel fibers enhance the structural integrity of freshly printed layers, enabling higher vertical build without collapse or deformation [47, 53]. This is crucial in 3D printing, where the material must support subsequent layers. External assisted fiber orientation may be beneficial for reinforcement at the interfaces between layers, minimizing weak planes and delamination issues, which often occur in layered extrusion-based printing [41]. By bridging cracks and delaying crack propagation, steel fibers significantly improve flexural and tensile performance, enhancing the overall ductility and toughness of the printed elements [47, 54]. The ability of steel fibers to bridge micro- and macro-cracks allows the material to absorb and dissipate more energy during loading, making it more resistant to dynamic and impact forces. However, these mechanical gains are counterbalanced by challenges in fresh-state properties. Increased fiber content raises yield stress and reduces flowability, reducing extrudability and risking nozzle blockage during printing.

Steel fibers address both fresh-state challenges (buildability and layer stability) and mechanical property

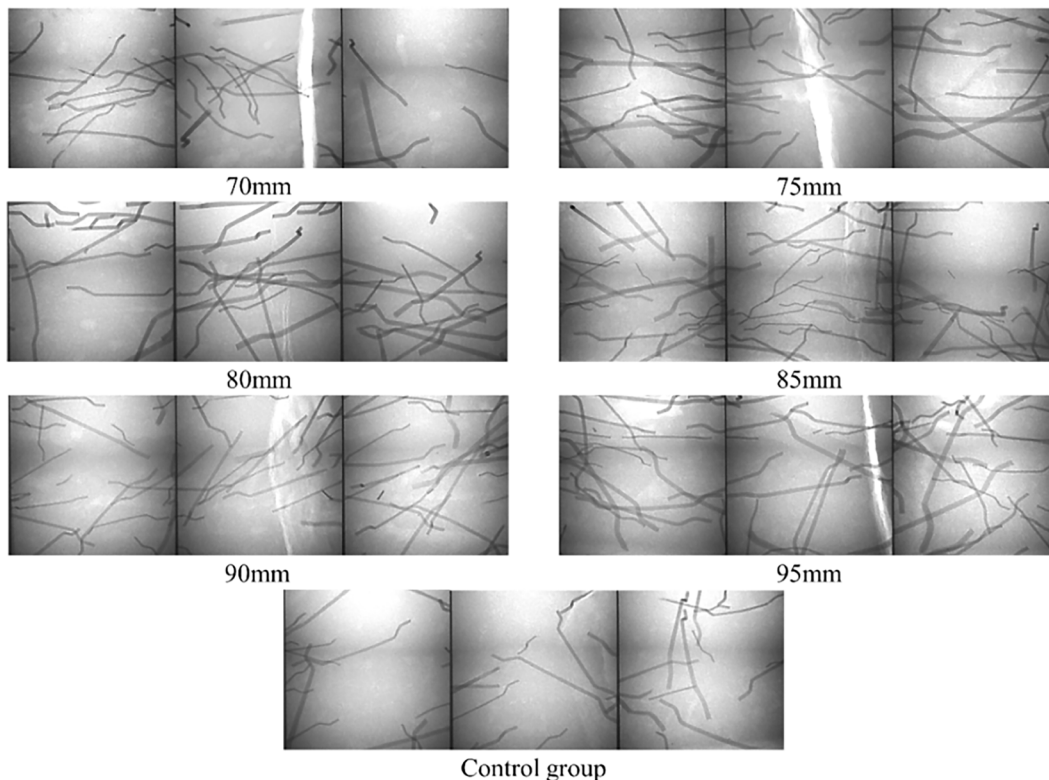


**Figure 23:** Fiber alignment under varying magnetic field intensities [41].



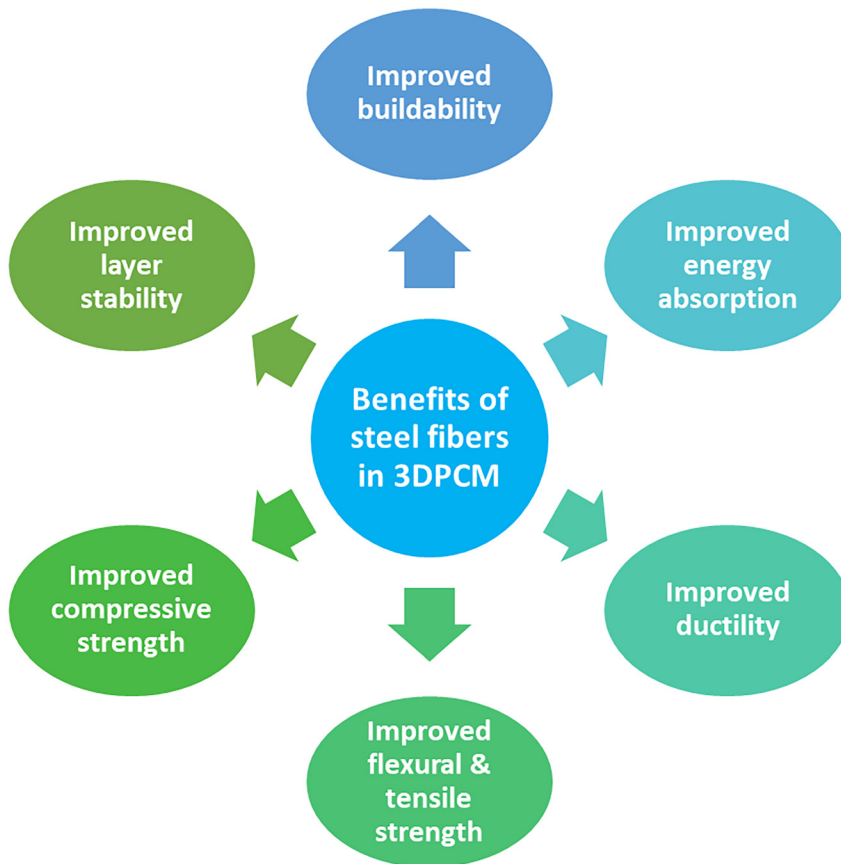


**Figure 24:** Summary of steel fibers advantages in 3DPCM.

enhancements (strength, ductility, energy absorption) in hardened 3D-printed structures. This dual contribution makes them particularly valuable in advancing structural-scale additive manufacturing with concrete, where achieving both print quality and long-term durability is critical. While steel fibers present clear reinforcement benefits in 3DPCM, their effectiveness depends heavily on dosage optimization, fiber orientation control, and synergy with printing process parameters.

## 7 Conclusions

This review underscores the pivotal role of steel fiber reinforcement in enhancing the performance of 3DPCM. The following conclusions can be drawn from the compilation of published literature:

- Adding steel fibers decreases flowability due to mechanical interlocking and fiber bridging, with longer fibers having a more pronounced effect. The best results are usually at 1–2 % fiber content. Higher amounts cause problems like nozzle blocking and uneven filaments.
- Both static and dynamic yield stress are increased with fiber dosage increase, which benefits buildability but results in reduced extrudability at higher fiber contents.
- Printability of 3DPCM is highly sensitive to fiber content and geometry. Incorporation of steel fibers in moderate quantity (typically 0.5–2.0 vol%) enhances shape stability and buildability, while excessive contents (>2.5 vol%) result in nozzle clogging.
- Steel fibers significantly enhance the compressive and flexural strengths of 3DPCM compared to plain 3DPCM, with more pronounced improvements observed in flexural strength due to effective crack-bridging. However, these improvements are highly dependent on loading direction, showing anisotropy due to the layer-by-layer deposition process.
- Plain 3DPCM displays brittle failure, but steel fibers change this to a more ductile response. They bridge cracks together, increase toughness, and allow the material to carry load after the first crack.
- Extrusion-driven alignment favors fibers reinforcement along the print path but reduces interlayer resistance. Controlled toolpaths, rheological modifying, and magnetic

- field-assisted alignment offer promising solutions to reduce mechanical anisotropy.
- Increased fibers content generally results in better mechanical properties but worsens the printability. A balance is needed, with 1–2 % fiber content identified as the most practical range.

## 8 Future recommendations

As 3D concrete printing is a relatively new research area, extensive studies are required to standardize laboratory procedures for evaluating 3DPCM characteristics before practical implementation. The following recommendations are proposed for future research:

- Investigate optimal combinations of fiber size and content to enhance mechanical strength without compromising printability.
- Develop standardized testing methods for rheology, extrudability, and buildability to enable reliable comparison across studies.
- Explore orientation control techniques through tailored print toolpaths, external magnetic or electric fields, and hybrid reinforcement strategies combining fibers with continuous elements.
- Evaluate long-term durability aspects, including shrinkage, water penetration, and steel fiber corrosion, beyond short-term mechanical properties.
- Advance laboratory-scale research toward large-scale applications by addressing challenges in nozzle design for fiber-rich mixes, ensuring uniform fiber distribution, and formulate design standards suitable for field implementation.
- Explore steel fiber reinforcement in low-cement, high-admixture printable concretes by evaluating fiber interaction, dispersion, bonding, and rheological effects within optimized low-carbon matrices to enhance both sustainability and mechanical reliability of 3D-printed elements [60].
- Assess the life-cycle and performance implications of steel fibers in low-cement printable systems by investigating their impact on life-cycle cost, embodied carbon, and structural performance to determine whether fiber addition offsets or enhances the environmental benefits of binder reduction.
- Investigate the compatibility of steel fibers with internally cured limestone–calcined clay matrices by examining fiber performance, bonding, orientation, and printability in additive manufacturing to enhance durability and dimensional stability of sustainable 3D-printed composites [61].

- Examine steel fiber reinforcement in carbonatable and nano-modified ternary systems by investigating how fiber geometry, volume fraction, and orientation influence carbon capture potential, crack control, and post-crack toughness in cellulose nanocrystal-enhanced printable binders [62].

**Acknowledgments:** The research team thanks the Deanship of Graduate Studies and Scientific Research at Najran University for supporting the research project through the Nama'a program, with the project code (NU/GP/SERC/13/698-2).

**Funding information:** Graduate Studies and Scientific Research at Najran University for supporting the research project through the Nama'a program, with the project code (NU/GP/SERC/13/698-2).

**Author contribution:** Z. T: conceptualization, methodology, formal analysis, writing-original draft. Q. G: supervision, resources, writing, reviewing, and editing. A. A. A. E: data acquisition, validation, writing, reviewing, and editing. A. H. A: software, formal analysis, writing, reviewing, and editing. A. M. M: conceptualization, supervision, resources, methodology. M. A: software, visualization, formal analysis, validation, writing, reviewing, and editing. All authors have accepted responsibility for the entire content of this manuscript and approved its submission.

**Conflict of interest:** The authors state no conflict of interest.

**Data availability statement:** The dataset generated and/or analyzed during the current study are available from the corresponding author upon reasonable request.

## References

1. Buswell RA, da Silva WRL, Bos FP, Schipper HR, Lowke D, Hack N, et al. A process classification framework for defining and describing digital fabrication with concrete. *Cement Concr Res* 2020;134:106068.
2. Lloret-Fritsch E, Wangler T, Gebhard L, Mata-Falcón J, Mantellato S, Scotto F, et al. From smart dynamic casting to a growing family of digital casting systems. *Cement Concr Res* 2020;134:106071.
3. Lowke D, Dini E, Perrot A, Weger D, Gehlen C, Dillenburger B. Particle-bed 3D printing in concrete construction – possibilities and challenges. *Cement Concr Res* 2018;112:50–65.
4. Buswell RA, Leal de Silva WR, Jones SZ, Dirrenberger J. 3D printing using concrete extrusion: a roadmap for research. *Cement Concr Res* 2018; 112:37–49.
5. Kamhawi A, Aghaei Meibodi M. Techniques and strategies in extrusion based 3D concrete printing of complex components to prevent premature failure. *Autom ConStruct* 2024;168:105768.
6. Farrokhsiar P, Gursoy B, Duarte JP. A comprehensive review on integrating vision-based sensing in extrusion-based 3D printing processes: toward geometric monitoring of extrusion-based 3D concrete printing. *Construction Robotics* 2024;8:21.

7. Perrot A, Rangeard D, Courteille E. 3D printing of earth-based materials: processing aspects. *Constr Build Mater* 2018;172:670–6.
8. Paolini A, Kollmannsberger S, Rank E. Additive manufacturing in construction: a review on processes, applications, and digital planning methods. *Addit Manuf* 2019;30:100894.
9. Zhang J, Wang J, Dong S, Yu X, Han B. A review of the current progress and application of 3D printed concrete. *Compos Appl Sci Manuf* 2019; 125:105533.
10. Kazemian A, Yuan X, Davtalab O, Khoshnevis B. Computer vision for real-time extrusion quality monitoring and control in robotic construction. *Autom ConStruct* 2019;101:92–8.
11. Habibi A, Buswell R, Osmari M, Aziminezhad M. Sustainability principles in 3D concrete printing: analysing trends, classifying strategies, and future directions. *J Build Eng* 2024;98:111354.
12. Batikha M, Jotangia R, Baaj MY, Mousleh I. 3D concrete printing for sustainable and economical construction: a comparative study. *Autom ConStruct* 2022;134:104087.
13. Rahul AV, Santhanam M, Meena H, Ghani Z. Mechanical characterization of 3D printable concrete. *Constr Build Mater* 2019;227: 116710.
14. Nan B, Qiao Y, Leng J, Bai Y. Advancing structural reinforcement in 3D-Printed concrete: current methods, challenges, and innovations. *Materials* 2025;18:252.
15. Sun J, Aslani F, Lu J, Wang L, Huang Y, Ma G. Fibre-reinforced lightweight engineered cementitious composites for 3D concrete printing. *Ceram Int* 2021;47:27107–21.
16. Li S, Khieu HH, Black JR, Nguyen-Xuan H, Tran P. Two-scale 3D printed steel fiber reinforcements strategy for concrete structures. *Constr Build Mater* 2025;458:139626.
17. Hopkins B, Si W, Khan M, McNally C. Recent advancements in polypropylene fibre-reinforced 3D-Printed concrete: insights into mix ratios, testing procedures, and material behaviour. *J Compos Sci* 2025; 9:292.
18. Li H, Addai-Nimoh A, Kreiger E, Khayat KH. Methodology to design eco-friendly fiber-reinforced concrete for 3D printing. *Cement Concr Compos* 2024;147:105415.
19. Si W, Hopkins B, Khan M, McNally C. Towards sustainable mortar: optimising sika-fibre dosage in ground granulated blast furnace slag (GGBS) and silica fume blends for 3D concrete printing. *Buildings* 2025; 15:3436.
20. Panda B, Paul SC, Tan MJ. Anisotropic mechanical performance of 3D printed fiber reinforced sustainable construction material. *Mater Lett* 2017;209:146–9.
21. Pham L, Tran P, Sanjayan J. Steel fibres reinforced 3D printed concrete: influence of fibre sizes on mechanical performance. *Constr Build Mater* 2020;250:118785.
22. Roussel N. Rheological requirements for printable concretes. *Cement Concr Res* 2018;112:76–85.
23. Tay YWD, Qian Y, Tan MJ. Printability region for 3D concrete printing using slump and slump flow test. *Compos B Eng* 2019;174:106968.
24. Perrot A, Rangeard D. 3D printing in concrete: techniques for extrusion/casting. *3D Printing of Concrete* 2019:41–72. <https://doi.org/10.1002/9781119610755.ch2>.
25. Lu B, Weng Y, Li M, Qian Y, Leong KF, Tan MJ, et al. A systematical review of 3D printable cementitious materials. *Constr Build Mater* 2019;207: 477–90.
26. Buswell RA, Soar RC, Gibb AG, Thorpe A. Freeform construction: mega-scale rapid manufacturing for construction. *Autom ConStruct* 2007;16: 224–31.
27. Weng Y, Li M, Tan MJ, Qian S. Design 3D printing cementitious materials via fuller Thompson theory and Marston-Percy model. *Constr Build Mater* 2018;163:600–10.
28. Lee SH, Kim HJ, Sakai E, Daimon M. Effect of particle size distribution of fly ash–cement system on the fluidity of cement pastes. *Cement Concr Res* 2003;33:763–8.
29. Le TT, Austin SA, Lim S, Buswell RA, Gibb AGF, Thorpe T. Mix design and fresh properties for high-performance printing concrete. *Mater Struct* 2012;45:1221–32.
30. Zhang C, Nerella VN, Krishna A, Wang S, Zhang Y, Mechtcherine V, et al. Mix design concepts for 3D printable concrete: a review. *Cement Concr Compos* 2021;122:104155.
31. Khan MA. Mix suitable for concrete 3D printing: a review. *Mater Today Proc* 2020;32:831–7.
32. L. Bing, “Mixture design and processing of novel spray-based cementitious materials for 3D printing,” PhD, School of Civil and Environmental Engineering, Singapore Centre for 3D Printing Nanyang Technological University; 2019. Available from: <https://dr.ntu.edu.sg/entities/publication/d668d0f4-32c2-4ba8-aad4-d93b249c86fc>.
33. Yang Y, Wu C, Liu Z, Zhang H. 3D-printing ultra-high performance fiber-reinforced concrete under triaxial confining loads. *Addit Manuf* 2022; 50:102568.
34. Pham L, Lu G, Tran P. Influences of printing pattern on mechanical performance of three-dimensional-printed fiber-reinforced concrete. *3D Print Addit Manuf* 2020;9:46–63.
35. Hassan A, Ilerioluwa G, Daniel EG, Marc H, Hassan N, Gabriel AA, et al. Studying steel fiber reinforcement for 3D printed elements and structures. *TX: Tran-SET*; 2022:299–309 pp.
36. Yang Y, Wu C, Liu Z, Wang H, Ren Q. Mechanical anisotropy of ultra-high performance fibre-reinforced concrete for 3D printing. *Cement Concr Compos* 2022;125:104310.
37. Giwa I, Game D, Ahmed H, Noorvand H, Arce G, Hassan M, et al. Performance and macrostructural characterization of 3D printed steel fiber reinforced cementitious materials. *Constr Build Mater* 2023;369: 130593.
38. Xia Z, Geng J, Zhou Z, Liu G. Comparative analysis of polypropylene, basalt, and steel fibers in 3D printed concrete: effects on flowability, printability, rheology, and mechanical performance. *Constr Build Mater* 2025;465:140098.
39. Altheoy F, Zaid O, Ahmed B, Elhadi KM. Impact of double hooked steel fibers and nano-kaolin clay on fresh properties of 3D-Printable ultra-high-performance fiber-reinforced concrete. *J Build Eng* 2024;97: 110917.
40. Jia Z, Zhou M, Chen Y, Wang W, Ma L, Chen Y, et al. Effect of steel fiber shape and content on printability, microstructure and mechanical properties of 3D printable high strength cementitious materials. *Case Stud Constr Mater* 2024;20:e03080.
41. Huang J, Peng Z, Tan X, Gong G, Yang H, Ren K, et al. Mechanism analysis of the magnetic field assisted 3D printed steel fiber reinforced concrete. *Constr Build Mater* 2025;458:139737.
42. Chu SH, Li LG, Kwan AKH. Development of extrudable high strength fiber reinforced concrete incorporating nano calcium carbonate. *Addit Manuf* 2021;37:101617.
43. Chen M, Li J, Zhang T, Zhang M. 3D printability of recycled steel fibre-reinforced ultra-high performance concrete. *Constr Build Mater* 2025; 462:139877.
44. Majain N, Rahman ABA, Mohamed RN, Adnan A. Effect of steel fibers on self-compacting concrete slump flow and compressive strength. *IOP Conf Ser Mater Sci Eng* 2019;513:012007.

45. Guerini V, Conforti A, Plizzari G, Kawashima S. Influence of steel and macro-synthetic fibers on concrete properties. *Fibers* 2018;6:47.
46. Cao G, Li Z, Jiang S, Tan Y, Li Z, Long S, et al. Experimental analysis and numerical simulation of flow behavior of fresh steel fibre reinforced concrete in magnetic field. *Constr Build Mater* 2022;347: 128505.
47. Zhang Y, Zhu Y, Ren Q, He B, Jiang Z, Van Tittelboom K, et al. Comparison of printability and mechanical properties of rigid and flexible fiber-reinforced 3D printed cement-based materials. *Constr Build Mater* 2023;400:132750.
48. Singh A, Liu Q, Xiao J, Lyu Q. Mechanical and macrostructural properties of 3D printed concrete dosed with steel fibers under different loading direction. *Constr Build Mater* 2022;323:126616.
49. Arunothayan AR, Nematollahi B, Khayat KH, Ramesh A, Sanjayan JG. Rheological characterization of ultra-high performance concrete for 3D printing. *Cement Concr Compos* 2023;136:104854.
50. Kazemian A, Yuan X, Cochran E, Khoshnevis B. Cementitious materials for construction-scale 3D printing: laboratory testing of fresh printing mixture. *Constr Build Mater* 2017;145:639–47.
51. Soltan DG, Li VC. A self-reinforced cementitious composite for building-scale 3D printing. *Cement Concr Compos* 2018;90:1–13.
52. Hou S, Duan Z, Xiao J, Ye J. A review of 3D printed concrete: performance requirements, testing measurements and mix design. *Constr Build Mater* 2021;273:121745.
53. Li H, Wei J, Khayat KH. 3D printing of fiber-reinforced calcined clay-limestone-based cementitious materials: from mixture design to printability evaluation. *Buildings* 2024;14:1666.
54. Arunothayan AR, Nematollahi B, Ranade R, Bong SH, Sanjayan J. Development of 3D-printable ultra-high performance fiber-reinforced concrete for digital construction. *Constr Build Mater* 2020;257:119546.
55. Arunothayan AR, Nematollahi B, Ranade R, Bong SH, Sanjayan JG, Khayat KH. Fiber orientation effects on ultra-high performance concrete formed by 3D printing. *Cement Concr Res* 2021;143:106384.
56. Shahzad Q, Abbas N, Akbar M, Sabi E, Thomas BS, Arshid MU. Influence of print speed and nozzle diameter on the fiber alignment in 3D printed ultra-high-performance concrete. *Front Mater* 2024;11:1355647.
57. Bos FP, Bosco E, Salet TA. Ductility of 3D printed concrete reinforced with short straight steel fibers. *Virtual Phys Prototyp* 2019;14:160–74.
58. Lesovik V, Fediuk R, Amran M, Alaskhanov A, Volodchenko A, Murali G, et al. 3D-printed mortars with combined steel and polypropylene fibers. *Fibers* 2021;9:79.
59. Zhou J, Lai J, Du L, Wu K, Dong S. Effect of directionally distributed steel fiber on static and dynamic properties of 3D printed cementitious composite. *Constr Build Mater* 2022;318:125948.
60. Bukhari SJS, Khanzadeh MM. Multicriteria performance assessment of ‘low w/c + low cement + high dosage admixture’ concrete: environmental, economic, durability, and mechanical performance considerations. *J Clean Prod* 2025;523:146419.
61. Bouchelil L, Shah Bukhari SJ, Khanzadeh Moradllo M. Evaluating the performance of internally cured limestone calcined clay concrete mixtures. *J Sustain Cem-Based Mater* 2025;14:198–208.
62. Al Fahim A, Bukhari SJS, Moradllo MK. Additive manufacturing of carbonatable ternary cementitious systems with cellulose nanocrystals. *Constr Build Mater* 2025;495:143753.